# Nano-YAG:Ce Mechanisms of Growth and Epoxy-Encapsulation

May Nyman, Lauren E. Shea-Rohwer,* James E. Martin, and Paula Provencio

*Sandia National Laboratories, P.O. Box 5800, Albuquerque, New Mexico 87185*

*Received November 18, 2008*

We have investigated the mechanism of nano-YAG:Ce growth in butanediol and glycol solvents. The static autoclave and low synthesis temperature (225 °C) that we employed provided conditions of slow growth in which we were able to observe an intermediate phase, a butanediol-intercalated layered alumina. This phase serves to passivate the surface in nano-YAG:Ce precipitates and thus contributes to increasing the quantum yield of YAG:Ce by diminishing surface effects such as Ce oxidation. While neat 1,4-butanediol results in precipitation of the nano-YAG:Ce, a mixture of 1,4-butanediol and diethylene glycol stabilizes a transparent colloid. We attribute this to higher solubility of the layered alumina intermediate in the solvent mixture and, thus, more homogeneous nucleation of the nano-YAG:Ce compared to heterogeneous nucleation in the neat 1,4-butanediol. However, the trade-off is slightly lower quantum yield in the transparent colloid, since the nano-YAG:Ce is not as thoroughly surface-passivated. With the transparent colloid, we were able to encapsulate the nano-YAG:Ce into a transparent epoxy dome that may be utilized in solid-state devices.

## Introduction

Cerium-doped yttrium aluminum garnet ($Y_3Al_5O_{12}:Ce^{3+}$, YAG:Ce) is the most commonly used phosphor in commercial white LEDs for solid-state lighting (SSL).[1,2] YAG:Ce absorbs blue light in the range of ∼440−460 nm and is thus ideal for excitation by blue InGaN LEDs. The combination of the blue light and the yellow-green YAG:Ce luminescence produces white light.[3,4] The overall conversion efficiency of white LEDs is only 30%, and to a large extent this low efficiency is attributable to the phosphor. Multiple scattering of the emission from the micrometer-sized phosphor powders leads to poor beam collimation, substantial backscattering of the emission into the semiconductor chip, and absorption losses in the phosphor itself. Particle scattering scales as the square of the particle mass, so reducing the particle size to the nanoscale would essentially eliminate scattering.

Oxide phosphors such as YAG:Ce are typically synthesized using solid state reactions that require annealing temperatures up to 1400 °C and result in large particle sizes. The synthesis of nanophosphors requires lower temperature methods in which the particles are nucleated, grown, and retained in solution, without aggregation. In general, the synthesis of oxide nanoparticles is hindered by the high lattice energy and low solubility of oxides in both aqueous and nonaqueous solvents. Problems specific to YAG:Ce synthesis include oxidation of $Ce^{3+}$ to $Ce^{4+}$ and competitive formation of kinetically more favorable yttrium aluminum oxide phases such as $YAlO_3$ perovskite and monoclinic $Y_4Al_2O_9$.[5−9]

Recently, there have been a few reports on the synthesis of nanometric YAG:Ce powders. For instance, combustion synthesis was used to produce ∼40 nm YAG:Ce powders at 600 °C.[10] The quantum yield (QY) of these powders was reported to be 54%[10] compared to ∼70% for commercial powders. A co-precipitation method was used to produce 20−30 nm undoped YAG powders.[11] Research led by Isobe[12−14] produced a rare example of synthesis of YAG:Ce by solution routes. Using a solvothermal method, nanoparticles of YAG:Ce (∼50 nm aggregates of 10 nm particles) were synthesized in 1,4-butanediol at 300 °C in a specialized stirred autoclave. The reported QY of these powders ranges from 21 to 38%. Isobe[15] also demonstrated transparency of a gel of the YAG:Ce nanoparticles by casting a film in an alcohol matrix. However, forming a robust nano-YAG:Ce

* To whom correspondence is to be addressed: leshea;@sandia.gov.

(1) Krames, M. R.; Shchekin, O. B.; Mueller-Mach, R.; Mueller, G. O.; Zhou, L.; Harbers, G.; Craford, M. G. *J. Disp. Technol.* **2007**, *3*, 160–175.
(2) Phillips, J. M.; Coltrin, M. E.; Crawford, M. H.; Fischer, A. J.; Krames, M. R.; Mueller-Mach, R.; G. O. Mueller, G.; Ohno, Y.; Rohwer, L. E. S.; Simmons, J. A.; Tsao, J. Y. *Laser Photonics Rev.* **2007**, *1*, 307–333.
(3) Jang, H. S.; Bin, I. W.; Lee, D. C.; Jeon, D. Y.; Kim, S. S. *J. Lumin.* **2007**, *126*, 371–377.
(4) Schlotter, P.; Schmidt, R.; Schneider, J. *Appl. Phys. A: Mater. Sci. Process.* **1997**, *64*, 417.
(5) Bhattacharyya, S.; Ghatak, S. *Trans. Ind. Ceram. Soc.* **2008**, *66*, 77–84.
(6) Mancic, L.; Rosario, G. D.; Marinkovic-Stanojevic, Z. V.; Milosevica, O. *J. Eur. Ceram. Soc.* **2007**, *27*, 4329–4332.
(7) Nyman, M.; Caruso, J.; Hampden-Smith, M. J. *J. Am. Ceram. Soc.* **1997**, *80*, 1231–1238.
(8) Tasi, M. S.; Fu, W. C.; Wu, W. C.; Chen, C. H.; Yang, C. H. *J. Alloys Compd.* **2008**, *455*, 461–464.
(9) Xia, L.; Qiang, L.; Jiyang, W.; Shunliang, Y. *J. Alloys Compd.* **2006**, *421*, 298–302.
(10) Haranath, D.; Chander, H.; Sharma, P.; Singh, S. *Appl. Phys. Lett.* **2006**, *89*, 173118.
(11) Wang, H.; Gao, L.; Niihara, K. *Mater. Sci. Eng. A.* **2000**, *288*, 1–4.
(12) Asakura, R.; Isobe, T.; Kurokawa, K.; Takagi, T.; Aizawa, H.; Ohkubo, M. *J. Lumin.* **2007**, *127*, 416–422.
(13) Kasuya, R.; Isobe, T.; Kuma, H. *J. Alloys Compd.* **2006**, *408*, 820–823.
(14) Kasuya, R.; Isobe, T.; Kuma, H.; Katano, J. *J. Phys. Chem. B* **2005**, *109*, 22126–22130.
(15) Kasuya, R.; Kawano, A.; Isobe, T. *Appl. Phys. Lett.* **2007**, *91*, 111916–111918.

10.1021/cm803137h CCC: $40.75 
Published on Web 04/02/2009

**Table 1. Summary of YAG:Ce Synthesis Experiments[a]**

| experiment | solution conditions[b] | product | quantum yield[c] |
|---|---|---|---|
| 1a | 100% 1,4-BD, 1% Ce | powder: YAG plus abundant layered alumina co-preciptate[d] | 57% |
| 1b | | powder: YAG plus minimal layered alumina co-precipitate[d] | 39% |
| 2 | 100% 1,4-BD, 3% Ce | powder: YAG plus layered alumina impurity | 40% |
| 3 | 100% 1,4-BD, 6% Ce | powder: YAG plus layered alumina impurity | 33% |
| 4 | 100% 1,3-BD, 1% Ce | powder: YAG | Faint blue emission (see text) |
| 5 | 95% 1,4-BD, 5% DEG, 1% Ce | powder: YAG | 51% |
| 6 | 95% 1,4-BD, 5% DEG, 3% Ce | powder: YAG | 22% |
| 7 | 95% 1,4-BD, 5% DEG, 6% Ce | powder: YAG | 16% |
| 8 | 90% 1,4-BD, 10% DEG, 1% Ce | powder: YAG | 39% |
| | | liquid: YAG | 44% |
| 9 | 90% 1,4-BD, 10% DEG, 3% Ce | powder: YAG | 50% |
| | | liquid: YAG | 44% |
| 10 | 90% 1,4-BD, 10% DEG, 6% Ce | powder: YAG | 47% |
| | | liquid: YAG | 45% |
| 11 | 87.5% 1,4-BD, 12.5% DEG, 1% Ce | powder: YAG | 35% |
| | | liquid: YAG | 38% |
| 12 | 85% 1,4-BD, 15% DEG, 1% Ce | powder: YAG | 29% |
| | | liquid: YAG | 41% |
| 13 | 80% 1,4-BD, 20% DEG, 1% Ce | amorphous powder | |
| 14 | 100% DEG, 1% Ce | amorphous powder | |

[a] All were heated for 4−7 days in a 24 mL Teflon Parr autoclave at 225 °C. BD = butanediol; DEG = diethyleneglycol. [b] % by weight. [c] 460 nm excitation wavelength. [d] See Figure 6.

monolith that may be incorporated into a solid-state device has not been reported.

In this work, we employ a variation of the solvothermal method using a static autoclave to produce transparent nano-YAG:Ce dispersions. The static autoclave, commonly known as a Parr reactor, is relatively inexpensive, extremely easy to use, and readily available in most materials synthesis laboratories. In contrast, the stirred autoclave used for Isobe's syntheses[12−14] is specialty equipment that is costly and found in few research laboratories. The goals of this study included (1) investigating the synthesis of nano-YAG:Ce utilizing the commonplace static Parr autoclave and comparing these syntheses to those performed by Isobe utilizing the stirred autoclave; (2) optimizing the solution chemistry for the static autoclave so that YAG:Ce nanoparticle dispersions are produced, and (3) producing a robust monolith composed of transparent dispersions of YAG:Ce encapsulated in an epoxy resin. The products obtained in the static autoclave differed in morphology, phase, and luminescent behavior (quantum yield) from those obtained in the stirred reactor, reported by Isobe. Varying both quantum yield and dispersibility of nano-YAG:Ce as a function of reaction conditions provided insight into the mechanism of formation of the nano-YAG:Ce, as well as a means to optimizing both the quantum yield and the dispersibility.

## Experimental Section

**Synthesis of Nano-YAG:Ce.** The synthesis used in this work is a variation of that reported in refs 12−14. In a typical reaction, yttrium and cerium acetate hydrate (Aldrich) and aluminum isopropoxide (Acros) were mixed together in a solvent such as 1,4-butanediol (1,4-BD) from Acros; 1,3-butanediol (1,3-BD) from Aldrich or diethylene glycol (DEG) from Fisher. In general, a 23 mL Teflon vessel for a Parr reaction vessel was used for these syntheses. Ten milliliters of solvent (1,4-BD, 1,3-BD, or a mixture of 1,4-BD plus DEG), 0.39 g of yttrium acetate (1.47 mmol), 0.5 g of aluminum isopropoxide (2.45 mmol), and 0.005, 0.015, or 0.030 g of cerium acetate (0.016 mmol, 0.048 mmol, or 0.096 mmol) were stirred in the Teflon Parr vessel with mild heating for ∼0.5 h on a hot plate to homogenize the mixture. The reaction vessel was then closed and placed in a 225 °C oven for 4−14 days. Experiments are summarized in Table 1. Precipitated solids were isolated by centrifugation at 3500 rpm and then washed and filtered with methanol. For some of the mixed 1,4-BD−DEG solvent systems, the samples required centrifugation at 10 000 rpm to settle the very finely dispersed powders.

**Encapsulation of Nano-YAG:Ce.** A solvent exchange process was developed to disperse the nano-YAG:Ce nanoparticles in an epoxy resin. The nano-YAG:Ce dispersions in 90% 1,4-BD-10% DEG were centrifuged at 6000 m/s$^2$. The supernatant was then decanted, and the nanoparticles were redispersed in tetrahydrofuran (THF). This solvent exchange process was repeated several times to substantially remove the original nonvolatile solvent, resulting in a dispersion of nano-YAG:Ce in THF, which is quite volatile, with a vapor pressure of 129 torr at ambient temperature.

In a second step this solvent exchange process was repeated, but the second "solvent" was the epoxy resin EPON 815C (Hexion specialty chemicals). The final dispersion of YAG:Ce in the epoxy was then rotoevaporated at 60 °C to remove any residual THF. The amine curing agent (Jeffamine−Hexion specialty chemicals) was then added, and the thoroughly mixed prepolymer resin was cured overnight at 55 °C to yield encapsulated nanoparticles for optical studies.

**Characterization of YAG Powders and Stable Colloids.** The nano-YAG:Ce precipitates were characterized by powder X-ray diffraction and infrared spectroscopy. X-ray powder diffraction was performed with a Bruker D8 Advance diffractometer in Bragg−Brentano geometry with Ni-filtered Cu Kα radiation. Infrared spectra (400−4000 cm$^{-1}$) were recorded on a Thermo Nicolet 380 FT-IR equipped with a Smart Orbit (Diamond) ATR accessory. Both the precipitated and dispersed YAG:Ce nanoparticles were examined using transmission electron microscopy (TEM) and energy dispersive spectroscopy. The samples were prepared by very light grinding in a mortar/pestle and then covered with water. A TEM grid was placed at the bottom of the mortar, and the sample was swirled resulting in a TEM grid with abundant small pieces of sample. TEM was done first on a JEOL 1200 EX with Gatan slow scan imaging at Sandia. HRTEM was done on a JEOL 2010 F with Gatan energy filtered imaging, in the High Resolution Microscope User Facility at UNM in Earth and Planetary Science Department. Energy Dispersive Spectroscopy was used via TEM or SEM to

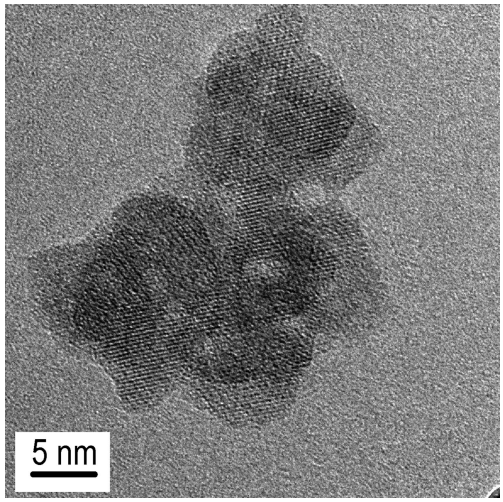


**Figure 1.** High-resolution TEM image of an aggregate of precipitated nano-YAG:Ce.

determine the doping levels of Ce in the YAG powders, via the ratio of Ce:Y, compared to a known standard. These analyses revealed that the doping levels were approximately the same as the amount provided in the synthesis; thus, the doping levels are referred to as the 1, 3, and 6% of the synthesis. To determine whether the nanoparticles form aggregates in solution, quasi-elastic light scattering (QELS) was used to measure the translational diffusion coefficient of the dispersed particles or aggregates. From this measured diffusion coefficient the hydrodynamic particle diameter was calculated using the Stokes−Einstein relation.

**Photoluminescence (PL) Measurements.** The PL emission and excitation spectra were collected using a Horiba Jobin-Yvon Fluorolog-3 double-grating/double-grating fluorescence spectrophotometer. Liquid samples were placed in 1-cm path length square cuvettes and excited with 460 nm light. The emitted light was detected at 90° from the incident beam. Powder measurements were made by orienting the sample 11° from the incident beam and detecting the emitted light from the front face of the sample. The excitation spectra were collected over the wavelength range of 275−500 nm, with the emission monitored at 550 nm. A complete instrumental correction was performed on all spectra that includes corrections for factors such as wavelength-dependent PMT response and grating efficiencies, among other factors. Absolute quantum yield measurements were made by exciting the samples with diffuse light inside an integrating sphere.[16]

## Results

**Synthesis.** Using a solution synthesis method we have produced nano-YAG:Ce powders and dispersions at significantly lower temperatures than those required to produce the bulk material and 75 °C lower than that reported by Isobe et al. for synthesis of nano-YAG:Ce powders. The choice of solvent system has a profound effect on the phase and state (precipitate vs stable colloid) of the product. Below, syntheses in different solvents are described; these results are also summarized in Table 1.

*1,4-Butanediol.* Synthesis in 1,4-butanediol (1,4-BD) results in YAG:Ce precipitates, such as those shown in the high-resolution TEM image of Figure 1, revealing 5 nm nanoparticles aggregated in 10−100 nm clusters. There is also a layered alumina phase present, discussed further below. Infrared analysis of the precipitate showes 1,4-BD to be present in the precipitate: the bands marked 1,4-BD in Figure 2 correlate exactly with a spectrum of neat 1,4-BD. The acetate ligands are also present, as observed by Isobe. Since no isolated YAG nanoparticles remain suspended in the 1,4-BD solution (as determined by no yellow color, no glow under a UV-lamp), we initially concluded that the formation of the YAG precipitate might be aided by 1,4-BD tethering the YAG nanoparticles. In an attempt to prevent YAG aggregation, we performed syntheses of nano-YAG:Ce in closely related diols such as 1,3-butanediol (1,3-BD), 1,4-pentanediol, and 1,5-pentanediol. We were surprised to find that all of these solvents, except 1,3-BD, led to an amorphous product.

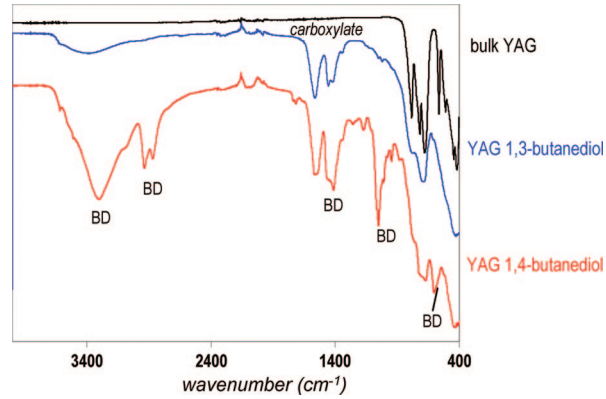


**Figure 2.** Infrared spectra of nano-YAG:Ce from 1,3-butanediol and 1,4-butanediol and bulk YAG:Ce powder for comparison. The peaks marked BD correspond to 1,4-butanediol.

*1,3-Butanediol.* Although the product formed in 1,3-BD was nanocrystalline YAG, it does not emit the yellow-green $Ce^{3+}$ luminescence. Infrared analysis of the nano-YAG from 1,3-BD *does not* indicate butanediol present in the precipitate. Rather, the acetate ligands from the yttrium acetate are associated with the surface of the product. Like many organic solvents, the 1,3-BD turned orange in color upon heating and emits a blue glow under a UV lamp. This glow appears to mask any weak emission from the Ce-doped YAG. Furthermore, the dark color of the solvent indicates redox reactions, which likely resulted in oxidation of $Ce^{3+}$ to $Ce^{4+}$. On the other hand, the 1,4-BD remains colorless; even after extensive heating, even with diethylene glycol added (see below). This unusual stability of 1,4-butanediol among common organic solvents renders it uniquely exceptional as a medium for these redox-sensitive syntheses.

*Diethylene Glycol.* Reactions in pure diethylene glycol (DEG) resulted in nonluminescent precipitates. However, when DEG is used as a co-solvent with 1,4-BD, a range of products is formed, as described below.

*1,4-Butanediol and Diethylene Glycol Co-Solvent.* While synthesis in neat 1,4-butanediol results in only precipitates of nano-YAG:Ce, the addition of DEG as a co-solvent in the range of 10−15% vol % results in a product that is a stable, transparent solution of dispersed YAG:Ce nanoparticles. Increasing the DEG to 20 vol % resulted in an amorphous, nonluminescent product, and decreasing the DEG to 5 vol % resulted in YAG:Ce precipitate only (no colloidal

(16) Rohwer, L. S.; Martin, J. E. *J. Lumin.* **2005**, *115*, 77–90.

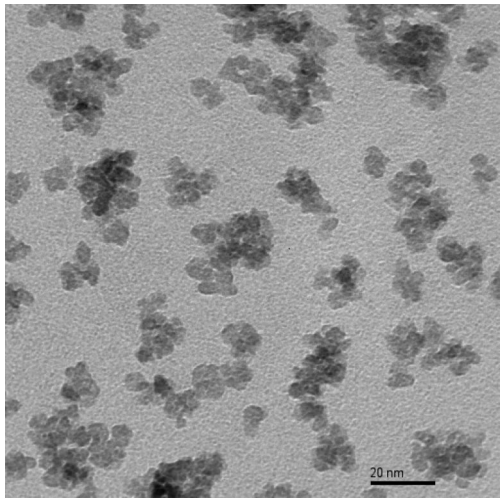


**Figure 3.** TEM micrograph of nanoparticles from the dispersion. When the solvent is evaporated for TEM sample preparation there is mild aggregation of the nanoparticles.

YAG:Ce). Solid YAG:Ce powders can be obtained by centrifuging viscous liquid colloids and repeated washing with ethanol followed by more centrifuging. X-ray diffraction analyses of these powders indicate the layered alumina is not present, but TEM analyses reveal otherwise (discussed further below). QELS measurements of the nano-YAG:Ce dispersions in 90% 1,4-BD/10% DEG gave an average aggregate size in solution of 96 nm. After this solution is centrifuged at 10 000 rpm the particle size in the supernatant is 9.6 nm, which is similar to the size of the primary particles shown in the TEM in Figure 3. When the supernatant is evaporated for TEM sample preparation there is mild aggregation of the nanoparticles, but this occurs during drying.

**Photoluminescence.** The photoluminescence (PL) emission and excitation spectra of nano-YAG:Ce precipitates and dispersions are comparable to those of bulk YAG:Ce. Figure 4a,b shows the PLE and PL for a nano-YAG:Ce dispersion synthesized in 90% 1,4-BD−10% DEG. The broad, yellow-green emission is due to the allowed electric dipole $4f^n-4f^{n-1}5d$ transitions of the $Ce^{3+}$ ions. The 5d excited state is localized and strongly influenced by the surrounding crystal field. YAG is a high band gap insulator so quantum confinement is not an issue, and achieving the proper emission does not require particle size control, as confirmed by these spectra. This is an advantage over semiconductor quantum dots whose charge carriers are delocalized, making them susceptible to luminescence quenching at surface states and emission spectral shifts due to the surrounding environment.

**Encapsulation.** We successfully encapsulated the nano-YAG:Ce in epoxy without quenching or shifting the nano-YAG:Ce emission. The PL emission spectrum of an optically transparent luminescent epoxy resin is shown in Figure 5a, and Figure 5b shows the YAG:Ce-epoxy dome excited under 460 nm. The transparency indicates good dispersion of the nanoparticles without agglomeration.

## Discussion

**Quantum Yield.** Absolute measurements show that the QY of the nano-YAG:Ce precipitates is as high as 57% and

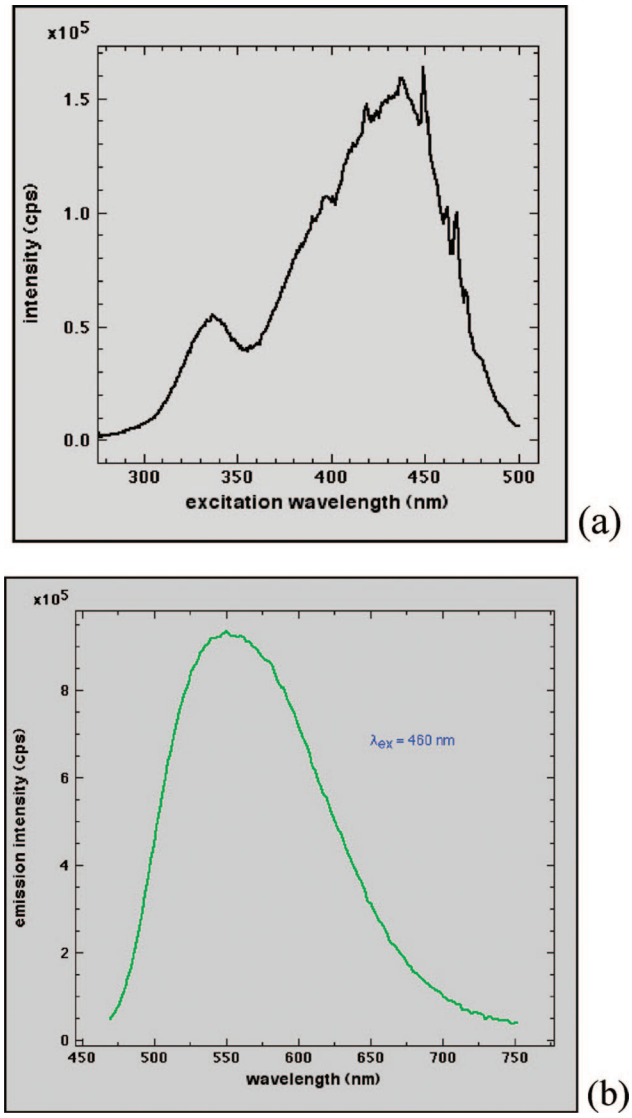


**Figure 4.** Photoluminescence of a nano-YAG:Ce dispersion: (a) excitation spectrum and (b) emission spectrum excited at 460 nm.

the transparent dispersions are as high as 45%. Isobe et al. reported nano-YAG:Ce precipitates with QYs of 21−38% made with the same cerium concentration (1%) as our samples. We investigated the effect of cerium concentration, solvent, and phase purity on the QY of nano-YAG:Ce and have compiled the results in Table 1.

The effect of $Ce^{3+}$ concentration on the QY of the YAG precipitates and dispersions was studied at 1%, 3%, and 6% $Ce^{3+}$. For YAG precipitates synthesized in 100% 1,4-BD or a mixture of 95% 1,4-BD-5% DEG, the highest QY was obtained at a $Ce^{3+}$ concentration of 1%. This result agrees with that reported for concentration quenching studies in bulk YAG:Ce phosphors.[17,18] Increasing the $Ce^{3+}$ concentration decreased the QY, likely due to concentration quenching (Figure 6). Concentration quenching in nano-YAG:Ce has been observed by others[19] at $Ce^{3+}$

(17) Kang, Y. C.; Lenggoro, I. W.; Park, S. B.; Okuyama, K. *Mater. Res. Bull.* **2000**, *35*, 789–798.
(18) Yan, M. F.; Huo, T. C. D.; Ling, H. C. *J. Electrochem. Soc.* **1987**, *134*, 493–498.
(19) Pankratov, V.; Millers, D.; Grigorjeva, L.; Lojkowski, W.; Kareiva, A. *Funct. Mater. Nanotechnol.* **2007**, *93*, 1–9.

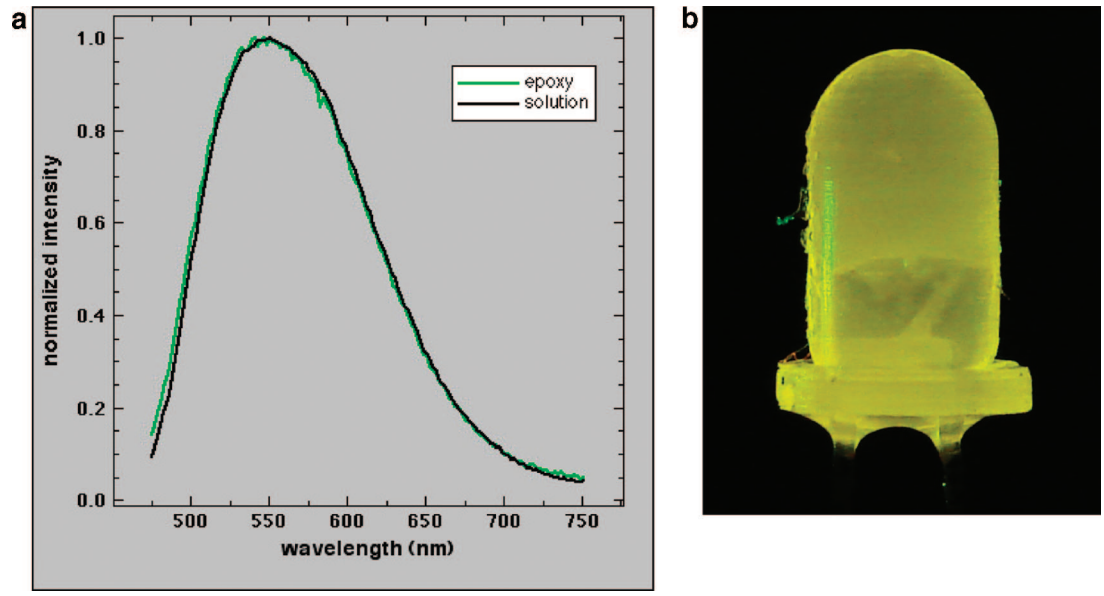


**Figure 5.** (a) Photoluminescence of nano-YAG:Ce in epoxy and in solution. The nano-YAG:Ce emission properties are preserved in the epoxy. (b) Photograph of the YAG:Ce-epoxy dome excited at 460 nm.

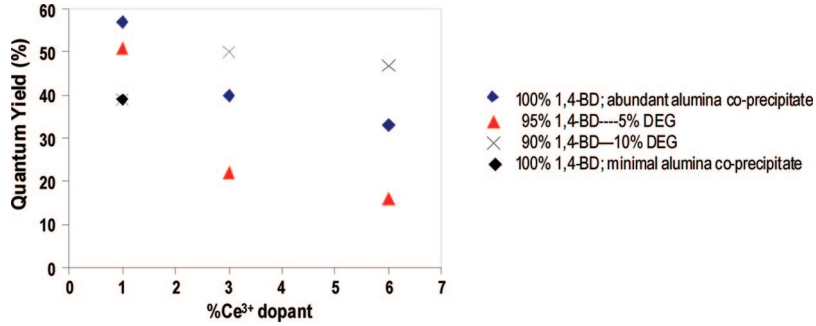


**Figure 6.** Quantum yield as a function of $Ce^{3+}$ concentration for nano-YAG:Ce precipitates obtained from different 1,4-BD−DEG ratios.

concentrations >0.5% when excited with VUV wavelengths at low temperature (10 K).

The addition of 10% DEG to 1,4-BD resulted in nano-YAG:Ce precipitates and dispersions with concentration quenching behavior different from that of the other precipitates. The QY of these nano-YAG precipitates was highest at 3% $Ce^{3+}$, with a decrease in the QY at 6% $Ce^{3+}$.

The nano-YAG synthesized by Isobe[12−14] in 1,4-BD is surface-complexed with acetate, whereas we clearly observed both 1,4-BD and acetate present, as indicated by infrared spectroscopy (Figure 2). Isobe obtained a QY of 22% for nano-YAG doped with 1% $Ce^{3+}$ from neat 1,4-BD, and we obtained QYs ranging from 39−57% (see Table 1). While it was initially assumed that surface capping with 1,4-BD is responsible for the increased QY since it is observed by IR, we have concluded that a layered alumina co-precipitate plays a significant role.

We characterized two nano-YAG:Ce precipitates from a single reaction (experiment 1a and 1b in Table 1). The precipitate from experiment 1a has a QY of 57% and contains an abundant alumina-rich layered co-precipitate (layer-spacing ~14 Å), as determined by X-ray diffraction (Figure 7). This product was a fine precipitate that required centrifugation at 3500 rpm to isolate it from the solvent. The precipitate from experiment 1b (QY = 39%) was collected without centrifugation—it was clearly denser than the precipitate of 1a, and settled on the bottom of the reactor. This was surprising because the 1b product clearly has a higher percentage of the YAG:Ce; conversely, 1a clearly has a higher percentage of the layered alumina.

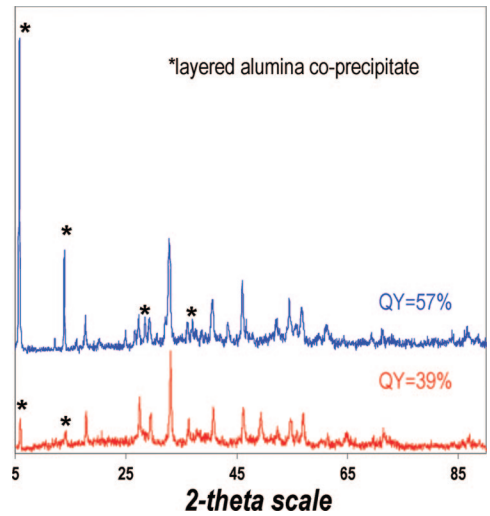


**Figure 7.** X-ray diffraction patterns for nano-YAG:Ce precipitates obtained from pure 1,4-BD in experiments 1a and 1b (Table 1) showing YAG and alumina diffraction peaks. Precipitates with higher quantum yield contain more alumina co-precipitate.

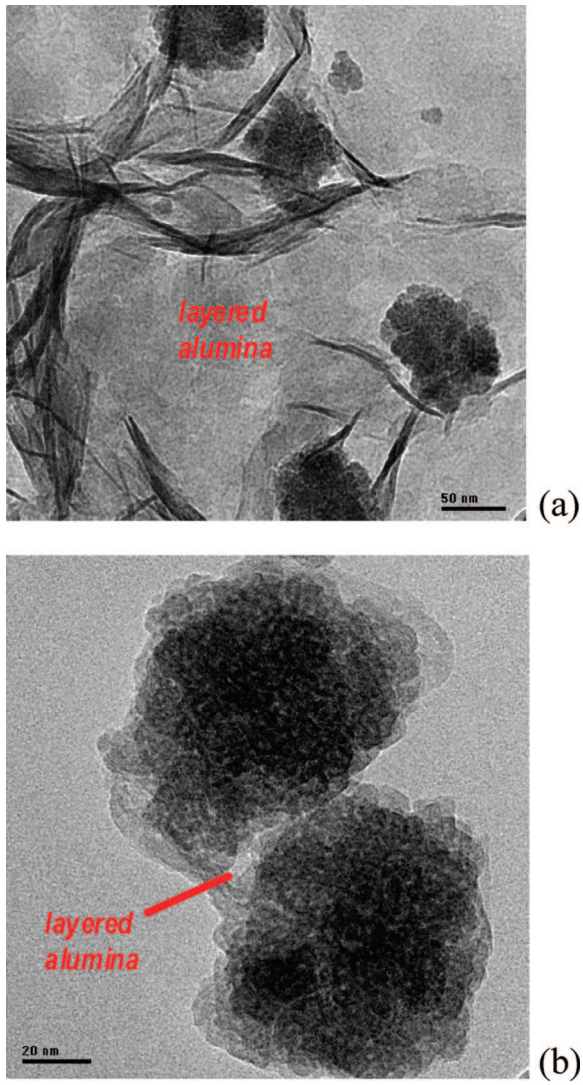


**Figure 8.** (a, b) TEM micrographs of nanoparticle aggregates and the alumina co-precipitate.

Although we detected the alumina phase by X-ray diffraction only in the 100% 1,4-BD products, it was identified by TEM imaging of powders obtained from the mixed DEG−1,4-BD solvent systems. Figure 8 shows nano-YAG:Ce aggregates that are in contact with, or enmeshed in, the alumina precipitate. By TEM, the alumina precipitate was identified by its layered morphology and its composition by energy dispersive spectroscopy (no yttrium, no cerium; containing aluminum and oxygen only). Finally, we carried out a control experiment where the synthesis in 1,4-BD was executed without the yttrium and cerium precursors (only aluminum). This experiment did result in the formation of a layered (as determined by X-ray diffraction) alumina phase with butanediol (identified by IR) present, most likely in the interlayer space. The layer spacing is ∼12 Å rather than the 14 Å observed in YAG−alumina mixtures. This can be due to differences in tilt angle of the butanediol relative to the alumina layers, different degrees of hydration, or differences in structure within the alumina slabs. The 12 Å *d*-spacing exactly matches that of butanediol-intercalated kaolinite.[20] Since the 1,4-BD is observed by IR both

(20) Murakami, J.; Itgaki, T.; Kuroda, K. *Solid State Ionics* **2004**, *172*, 279–282.

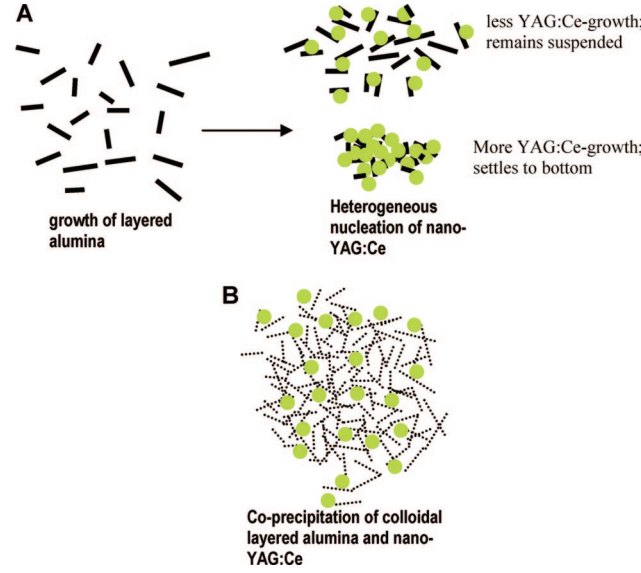


**Figure 9.** Schematic of the formation of layered alumina and nano-YAG:Ce in (A) 1,4-butanediol where the layered alumina is an insoluble intermediate that serves as a template for nano-YAG:Ce growth (see Table 1, experiments 1a and 1b) and (B) in 1,4-butanediol−diethyleneglycol where the layered alumina is more soluble and co-precipitates with the nano-YAG:Ce to form a stable colloid.

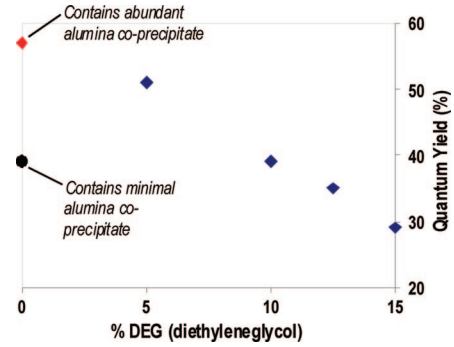


**Figure 10.** Quantum yield of nano-YAG:Ce precipitates as a function of diethylene glycol (DEG) content.

in the layered alumina without YAG:Ce and in the mixtures of layered alumina plus YAG:Ce but not in the YAG:Ce formed in 1,3-BD, we propose that the YAG:Ce formed in 1,4-BD is surface-passivated with 1,4-BD intercalated alumina rather than directly with the 1,4-BD. This may aid in preventing surface diffusion and/or oxidation of $Ce^{3+}$, which results in the increased quantum yield that we observe with increased layered alumina content in the precipitate.

The layered alumina was not observed in the stirred autoclave reactions of Isobe; the difference could arise either from the higher synthesis temperature (300 °C vs 225 °C) or the stirred vs static media. We suspect the differences are due more to the stirring than the temperature difference because the longer reaction times used in our studies likely compensated for the decreased reaction kinetics at our lower temperature: Isobe's experiments were complete in two hours, ours were heated for at least four days. In our static autoclave experiments, it is likely that the 1,4-BD-layered alumina phase is an intermediate product to the formation of YAG. This intermediate is relatively insoluble in the 1,4-BD, and thus the soluble yttrium and cerium acetates react with the surface of the layered alumina to nucleate growth

of the YAG:Ce. Furthermore, perhaps the layered alumina intermediate is more soluble in the 1,4-BD−DEG mixtures than in neat 1,4-BD, so the YAG:Ce is nucleated homogeneously from solution or from a more highly dispersed colloid rather than from an alumina precipitate. Thus, in the case of the 1,4-BD−DEG solvent mixtures, a more colloidal suspension is formed. These different growth mechanisms in 1,4-BD vs 1,4-BD−DEG are illustrated schematically in Figure 9. In summary, the result of increased alumina in the YAG:Ce precipitates is increased passivation of the YAG:Ce surface and increased quantum yield. On the contrary, QYs of YAG:Ce colloidal suspensions are relatively insensitive to parameters such as $Ce^{3+}$ concentration and DEG concentration. We suggest that these colloids all contain similar amounts of layered alumina passivating the YAG:Ce, and this has a greater effect on the QY than any other parameters.

## Conclusions

Solvothermal synthesis of nano-YAG:Ce that were carried out (1) in static autoclave conditions instead of stirred autoclave conditions and (2) at 75 °C lower reaction temperature than reported prior provided much information concerning the mechanism of nano-YAG:Ce formation in 1,4-butatnediol. Fortuitously, these studies also provide a means to increase the quantum yield of nano-YAG:Ce from 39% reported by Isobe and co-workers to 56%. We determined we could obtain YAG:Ce precipitates from neat 1,4-butanediol solutions that are surface-passivated with a layered alumina, which is largely responsible for the high QY. This layered alumina is an insoluble intermediate in the reaction process, and nano-YAG:Ce nucleates heterogeneously on its surface, forming a precipitate with high QY. When up to 10% diethyleneglycol is added to the reaction, the layered alumina intermediate is more soluble and the nano-YAG:Ce nucleates in a more homogeneous fashion such that it is retained in a stable colloidal state. Layered alumina is still present that partially passivates the surface but is not as abundant (resulting in the drop in QY to below 45%). With the nano-YAG:Ce formed under static autoclave conditions optimized for colloid stabilization and QY, we investigated encapsulation. We successfully epoxy-encapsulated nano-YAG:Ce into a transparent dome without change in the emission characteristics, which may be utilized in solid-state devices such as LEDs. Finally, the synthesis of nano-YAG:Ce reported here was carried out by an inexpensive method readily available in virtually any synthetic laboratory.

**Acknowledgment.** This work was funded by a grant from the United States Department of Energy National Energy Technology Laboratory (DE-PS26-06NT42942). Sandia is a multiprogram laboratory operated by Sandia Corporation, a Lockheed-Martin Company, for the United States Department of Energy under Contract No. DE-AC04-94AL85000.

CM803137H